3.B Rotational-Shearing Interferometry for Improved Target Characterization

Inertial-fusion targets have strict requirements regarding sphericity, surface smoothness, and layer-thickness uniformity. During fabrication, each target must be fully characterized to allow for the interpretation of experimental target shot data. We report here a new interferometric technique for the characterization of transparent targets.

Interferometric characterization techniques have been extensively used to measure target quality. An imperfect target, which can be described as a superposition of defects on a perfect spherical shell, produces an interferogram with the defect and perfect-shell components combined. It is often difficult to separate the defect-produced components in a target interferogram from the concentric fringe pattern produced by a perfect target; this limits precise interpretation of the target defects. We have used the rotational symmetry of a perfect target to improve defect-detection sensitivity by using rotational-shearing interferometry. One advantage of this approach is that rotationally symmetric objects produce null interferograms, making only the non-rotationally symmetric defects visible. Another advantage is that shell nonconcentricity can be measured independently of shell thickness. We have developed a simple analytical model which describes the interferometer's operation, and have constructed and tested a prototype device for fusion-target characterization.

Characterization of optically transparent target shells has generally been performed with interferometry.[1] The interferometers used have been primarily of the Twyman-Green,[2] Mach-Zehnder,[3] or lateral-shearing[4] configurations. Common to the operation of each of these instruments is the superposition and interference of the wave front passing through the target with a uniform plane wave front. The resultant interference pattern produced by a perfect target is a "bull's-eye" pattern rotationally symmetric about the target center. A non-axially symmetric target defect produces an asymmetry in the interference pattern, and measurement of this asymmetry has been the basis for characterizing the wall-thickness uniformity of targets. This approach has limitations because the defect-detection sensitivity is inversely proportional to target-shell thickness.[5] Thick target shells require a larger defect size for detectability.

The axial symmetry of inertial-fusion targets suggests the use of another interferometric characterization method, rotational-shearing interferometry. Here the wave front is passed through the target and then split into two parts; one part is rotated through an angle θ, and the two wave fronts are then recombined causing interference.[6] This technique has several advantages over conventional interferometry for fusion-target characterization. The detection sensitivity of shell-thickness nonuniformity has a fixed value. Also, the background bull's-eye pattern is not present, which makes local defects easier to detect. The most significant advantage of rotational-shearing interferometry is that it is an easily analyzed null test. A perfect fusion

target produces a uniform flat field, i.e., no fringe pattern is produced.

Various other types of interferometry have been developed that are also null tests. These have included flip-image,[7] 90° views,[7] and holographic[8] systems. Although these are usable as null tests, the interferograms produced are difficult to analyze.

Concept of Rotational-Shearing Interferometry

Rotational shearing superimposes a ray parallel to the z axis that intersects the target at (x,y) with a parallel ray passing through (x', y') (Fig. 29a). The relationship between these superimposed rays is given by a rotation about the z axis through an angle θ.

An x-z plane cut through a nonconcentric spherical shell having the defect axis aligned along the x axis is shown in Fig. 29b. The nonconcentricity Δt of the shell, defined as the distance separating the centers of the inner and outer spherical surfaces, can be obtained directly from rotational-shearing measurements. Neglecting refraction, a ray in the x-z plane passing through x, from $z = R_o$ to $z = -R_o$, has an optical path length (OPL) of:

Fig. 29
Configuration for rotational-shearing interferometry. A laser beam is passed through the glass shell parallel to the z axis, and is then split into two beams which are rotated through a relative angle of θ before being recombined to produce an interferogram. Rays intersecting the shell at x_1 and x'_1 will interfere with each other, as will rays at x_2 and x'_2. The nonconcentricity may be determined by counting fringes between adjacent points x_1 and x_2.

(a) X-Y Plane

T634

(b) X-Z Plane
(for $\theta = 180°$)
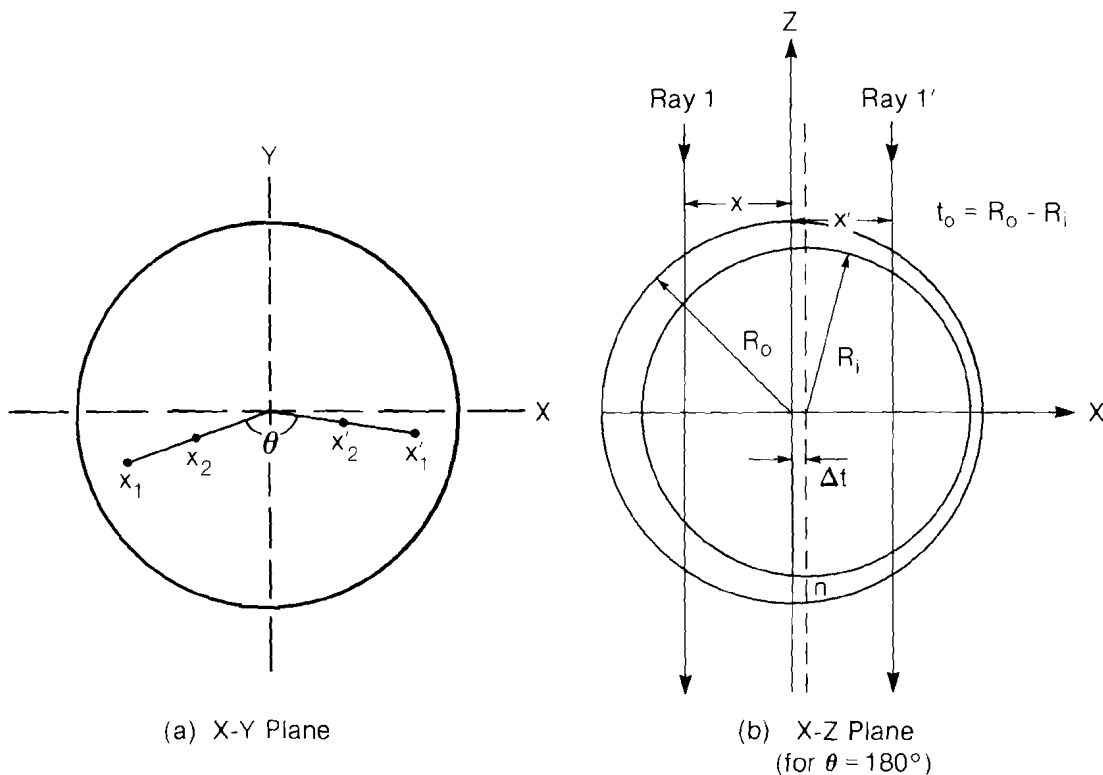
T567

$$OPL(x) = 2(n-1)\left\{ (R_o^2 - x^2)^{1/2} - [(R_o - t_o)^2 - (x - \Delta t)^2]^{1/2} \right\} + 2R_o \quad (1)$$

where n is the refractive index of the shell, R_o is the outer radius of the shell, t_o is the average shell thickness, and the refractive index interior and exterior to the shell is 1.0. Refraction is ignored here; a more detailed analysis shows that this omission does not lead to significant errors for small values of Δt.

Consider a second ray from the rotated image passing through (x', y') that is superimposed on the nonrotated ray. For the case $\theta = 180°$, x' = -x, and the difference in optical paths between the two nonrefracting rays, to first order in R_o^{-1}, is given by:

$$OPD(x) = OPL(x) - OPL(-x) = 2(n-1)\left(-\frac{2x\Delta t}{R_o} \right), \quad (2)$$

where it is assumed that

$$\frac{t_o}{R_o} << 1 \text{ and } \frac{x^2}{R_o^2} << 1.$$

The number of interference fringes produced between $(x_1,0)$ and $(x_2,0)$ is

$$m \equiv \left| \frac{OPD(x_1) - OPD(x_2)}{\lambda} \right| = \frac{4(n-1)}{\lambda} |x_1 - x_2| \frac{\Delta t}{R_o} \quad (3)$$

where λ is the wavelength of the light. Equation (3) can be inverted to give the nonconcentricity Δt directly from the number of fringes.

Lateral shear, introduced through misalignment of the target shell from the rotational axis of the interferometer, has been analyzed and found not to affect the nonconcentricity measurement to first order. Also, the shell thickness t_o does not appear in Eq. (3). This is in contrast with previous interferometric characterization techniques where $\Delta t \propto 1/t_o$.[5]

Orientation of the nonconcentricity defect in the x-y plane gives the greatest defect-detection sensitivity. Rotation of the defect axis away from the plane by an angle Φ decreases sensitivity to Δt by a factor of cos Φ.[2] In practice, the target shell can be oriented with $|\Phi| \leq 10°$, causing a decrease in sensitivity which is less than 3%.

Equation (3) expresses the relationship between shell nonconcentricity and interference measurements produced with 180° of rotational shear. Having the rotational-shear angle θ different from 180° reduces the nonconcentricity defect-detection sensitivity by $1 + \cos \theta$, which is small for θ near 180°. Aligning the rotation angle to within 10° of 180° presents no difficulties and reduces detection sensitivity by less than 3%.

Interferometer

Based on the encouraging results of the analytical model, an experimental apparatus was constructed. Figure 30 is a schematic of the instrument. The assembled interferometer, of the Mach-Zehnder configuration, uses matched components in each arm. The optical components were chosen so that only rotationally symmetric (spherical) aberration is introduced into each of the two beams. The aberrations are equal and cancel when the beams recombine. Plate beam splitters and dove prisms, which introduce astigmatism in a diverging wave front, were not used. Instead, beam splitting and rotation were performed with cube beam splitters and mirror-image rotators. Figure 31 is a photograph of the experimental rotational-shearing interferometer.

T477
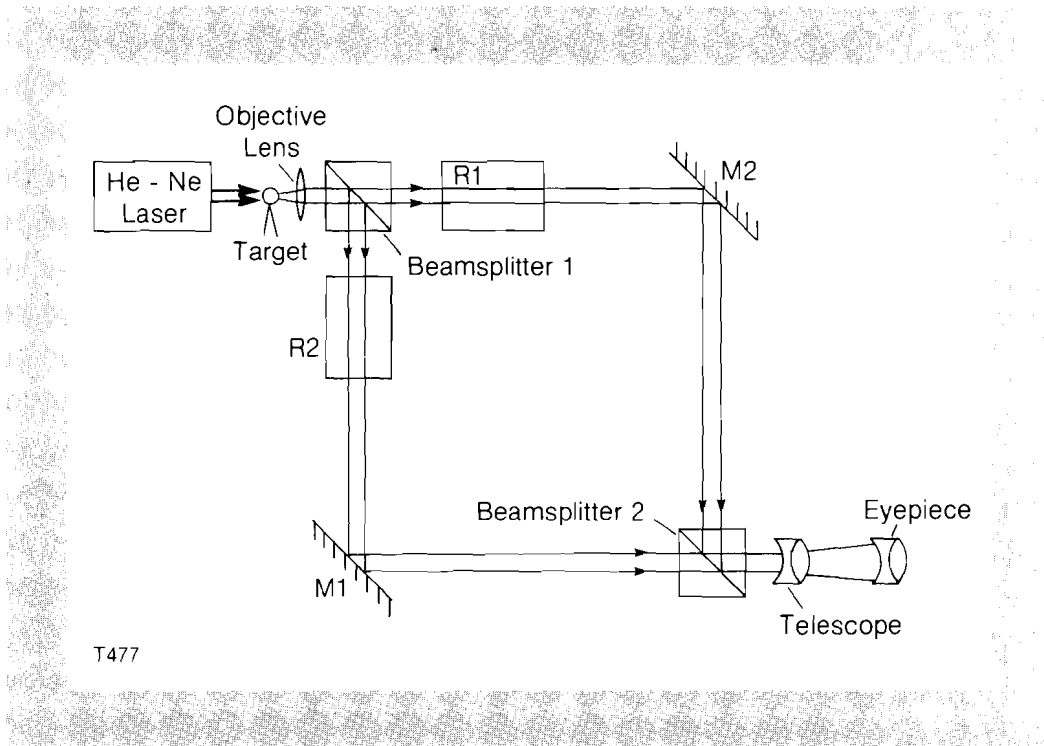
Fig. 30
Schematic of rotational-shearing interferometer.

The microscope objectives are corrected for use at infinite conjugates to ensure a minimum of image degradation from the long effective tube length of the microscope. A telescope assembly used at the interferometer's output cube beam splitter relays the image to the eyepiece.

The interferometer has approximately a half-wavelength of phase noise across its aperture. This arises primarily from defects in the cube beam splitters. Since this phase noise makes interpretation of small defects in targets difficult, two solutions were investigated to eliminate this problem. One involved using higher-quality optics in the interferometer, and the other involved operating the interferometer in an ac-phase-measurement mode. In the first case, the problem is minimized by reducing phase noise. In the second case, the noise is measured separately from the target and subtracted from the target measurement; this is the more desirable solution.

2 inches
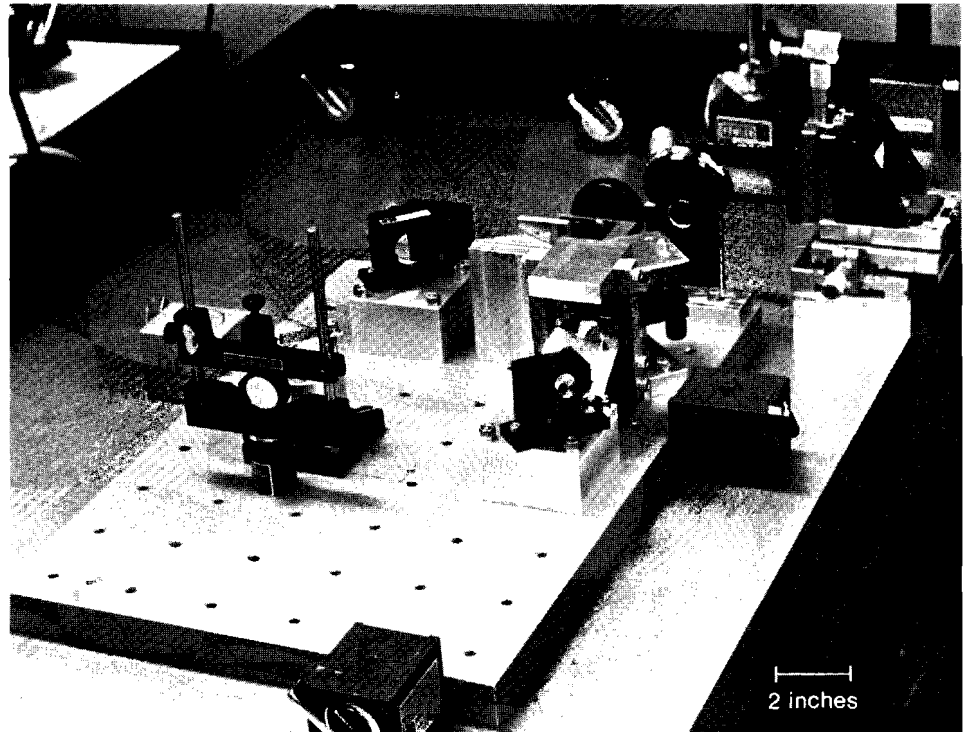
Fig. 31   T563
The rotational-shearing interferometric apparatus with objective lens at upper right.

Target-Shell Measurements

Targets are placed at the focal plane of the microscope's objective lens for characterization. The targets, supported either by a capillary stalk or by a microscope slide, are held by a precision micromanipulator having micrometer positioning capability. The two images from the interferometer are superimposed by moving the target to the rotation axis of the interferometer. Target images can be visually superimposed to ± 1% of their diameter.

The interferogram shown in Fig. 32a was produced by a target (350 μm in diameter, 3.4-μm shell thickness) that was displaced from the axis of rotation by a distance greater than its radius. With this degree of misalignment, the instrument operates like a lateral-shearing interferometer and produces two bull's-eye images similar to those from conventional interferometry.[2]

The interferogram in Fig. 32b was obtained from the same target, but using the rotational-shearing interferometer with less than $R_o/50$ misalignment of the two superimposed images. Here, parallel fringes perpendicular to the defect axis are evident. These can be used in Eq. (3) to quantify the degree of target-shell nonconcentricity. The measured fringe separation (m = 1) in Fig. 32b produced by 0.6328-μm light is 113 μm. The nonconcentricity calculated using Eq. (3) is $\Delta t = 0.5 \pm 0.05$ μm. This result was checked using the method of fringe-pattern decentration on Fig. 32a and found to agree to within 5%.[5]

Interferograms of a second target shell are shown in Figs. 32c and 32d. In Fig. 32c, the shell is displaced in the interferometer as in Fig.
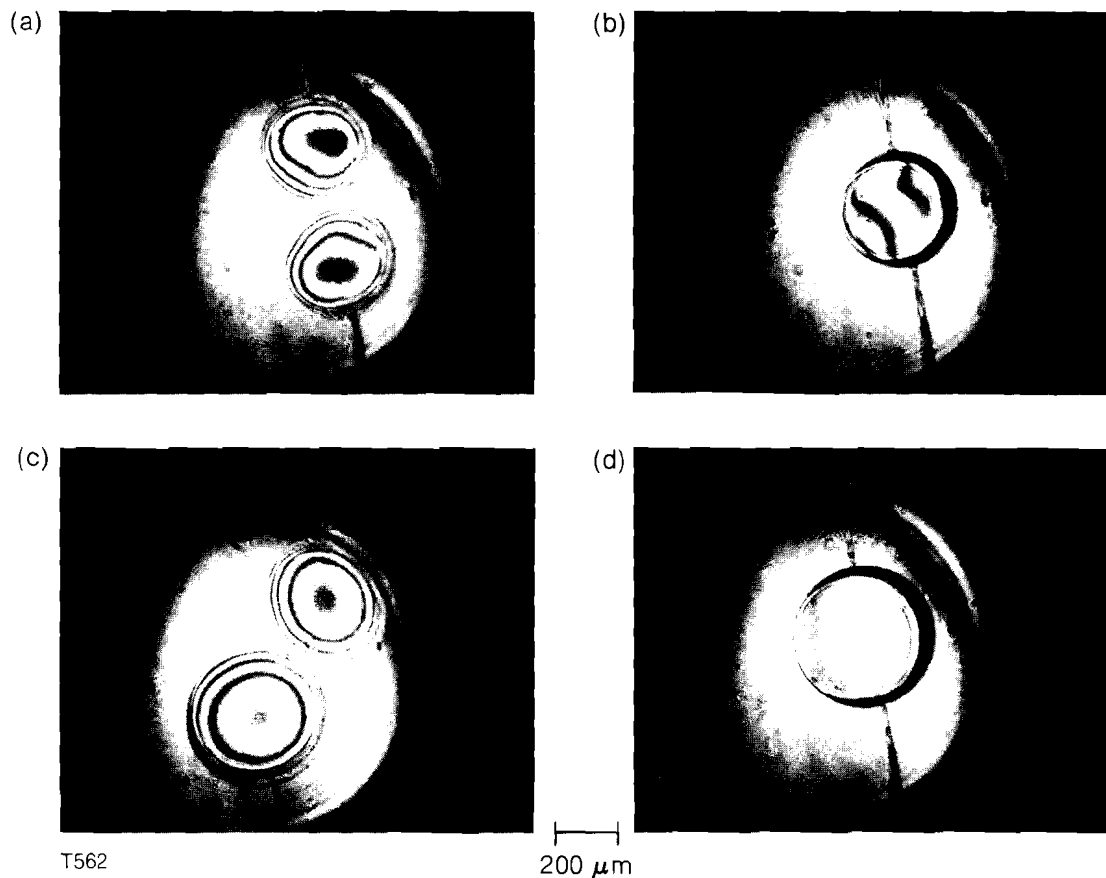
Fig. 32
Conventional total-shearing interfero-grams (left) and rotational-shearing inter-ferograms (right) of two stalk-mounted glass microballoons (top: 350-μm di-ameter; bottom: 425-μm diameter; both 3.4 μm thick). The rotational-shearing in-terferograms indicate nonconcentricities of 15% and <2% respectively.

32a, while in Fig. 32d, the images are superimposed with a minimum of lateral shear as in Fig. 32b. Figure 32d shows that this target has no detectable nonconcentricity defect; no detailed analysis is needed to interpret this interferogram. In contrast, it would be difficult to inter-pret the bull's-eye interference pattern of Fig. 32c.

Summary

A rotational-shearing interferometer offers distinct advantages for characterizing transparent inertial-fusion targets. The sensitivity of the instrument to nonconcentricity defects is independent of target-shell thickness, resulting in improved concentricity characterization of thick-walled targets. Since the device is inherently a null-test instru-ment, defects not easily visible using conventional target-characterization techniques can be readily recognized. This results because highly concentric shells do not produce the usual bull's-eye interference pattern. This apparatus appears to be well suited to analyzing fuel-layer uniformity in transparent cryogenic targets.

Additional work is needed to improve the performance of the instru-ment. The incorporation of wave-front-measuring techniques such as

ac interferometry would add to the sensitivity of the instrument and relax the quality requirements of the optical components. Another potential improvement involves varying the rotational-shearing angle θ. This would enable the instrument to locate and measure defects other than nonconcentricity.

REFERENCES

1. B. W. Weinstein, *J. Vac. Sci. Technol.* **20**, 1349 (1982).

2. R. R. Stone, D. W. Gregg, and P. C. Souers, *J. Appl. Phys.* **46**, 2693 (1975).

3. P. O. McLaughlin and D. T. Moore, *J. Opt. Soc. Am.* **67**, 1386 (1977).

4. J. R. Miller and J. E. Sollid, *Appl. Opt.* **17**, 852 (1978).

5. T. F. Powers, *J. Vac. Sci. Technol.* **20**, 1355 (1982).

6. M. V. R. K. Murty and E. C. Hagerott, *Appl. Opt.* **5**, 615 (1966).

7. B. W. Weinstein, H. Medecki, J. A. Monjes, R.M. Singleton, and D.L. Willenborg, Lawrence Livermore 1978 Annual Report, UCRL-50021-78, 4-31, 1979.

8. T. P. Bernat, D. H. Darling, and J. J. Sanchez, *J. Vac. Sci. Technol.* **20**, 1362 (1982).